LiOH and NaOH molecules, whereas minimum flattening (0·13–0·11 Å) is found in LiH and NaH molecules.

Of course one must account for the environment surrounding the isolated molecules if one wants to compare the present theoretical results with real systems in the crystals. Such theoretical approaches are now scheduled.

The authors thank Dr Michael Schmidt, North-Dakota State University, who kindly provided them with the North-Dakota version of *GAMESS* program. A special debt of gratitude goes to our mentors: Professor N. S. Hush and G. Bacskay, The University of Sydney, who introduced us to these areas.

References

BADER, R. F. W., CARROL, M. T., CHEESEMAN, J. R. & CHANG, C. (1987). *J. Am. Chem. Soc.* **109**, 7968–7979.

BADER, R. F. W., HENNECKER, W. N. & CADE, P. E. (1967). *J. Chem. Phys.* **46**, 3341–3363.

BOYD, R. J. & WANG, L.-C. (1989). *J. Comput. Chem.* **10**, 367–375.

DUPUIS, M., SPANGLER, D. & WENDOLSKI, J. J. (1981). *NRCC Software Catlog* (*QG*01). Lawrence Berkeley Laboratory, Univ. of California, USA.

GORDON, M. S. (1980). *Chem. Phys. Lett.* **76**, 163–168.

HARIHARAN, P. C. & POPLE, J. A. (1973). *Theor. Chim. Acta*, **28**, 213–222.

HEHRE, W. J., DITCHFIELD, R. D. & POPLE, J. A. (1972). *J. Chem. Phys.* **56**, 2257–2261.

IKUTA, S. (1989*a*). *J. Mol. Struct. Theochem.* In the press.

IKUTA, S. (1989*b*). Submitted.

KRISHNAN, R., BINKLEY, J. S., SEEGER, R. & POPLE, J. A. (1980). *J. Chem. Phys.* **72**, 650–654.

MCLEAN, A. D. & CHANDLER, G. S. (1980). *J. Chem. Phys.* **72**, 5639–5648.

NYBURG, S. C. & FAERMAN, C. H. (1985). *Acta Cryst.* B**41**, 274–279.

PEARSON, R. G. (1988*a*). *J. Am. Chem. Soc.* **110**, 7684–7690.

PEARSON, R. G. (1988*b*). *Inorg. Chem.* **27**, 734–740.

SCHMIDT, M. (1989). North-Dakota version of *GAMESS* program. North Dakota State Univ., USA.

Acta Cryst. (1990). B**46**, 27–39

Bonding-Deformation and Superposition Effects in the Electron Density of Tetragonal Nickel Sulfate Hexadeuterate $NiSO_4.6D_2O$

BY G. J. MCINTYRE,* H. PTASIEWICZ-BAK† AND I. OLOVSSON

Institute of Chemistry, University of Uppsala, Box 531, *S*-751 21 *Uppsala, Sweden*

(*Received* 19 *May* 1989; *accepted* 18 *September* 1989)

Abstract

The electron density in the title compound has been determined at room temperature by multipole refinement against single-crystal X-ray intensity data. Hydrogen positional and displacement parameters were fixed to values determined by refinement against single-crystal neutron data. The electron density based on the deformation functions of all atoms in the structure is compared with the individual densities calculated from the deformation functions of only nickel or the separate water molecules. In this way the effects of simple superposition of the individual densities have been studied. The experimental deformation density around nickel is in good agreement with that expected from simple ligand-field theory for an ideally octahedral $Ni(D_2O)_6^{2+}$ complex. The individual densities of the water molecules show clear polarization of the lone-pair densities according to the coordination of the water molecules. This polarization is distorted by superposition in the electron density based on all atoms; in particular, the apparent decrease of the electron density in the lone-pair regions of the water O atoms can be attributed to superposition of the oxygen density with the negative deformation density of nickel. Crystal data: $NiSO_4.6D_2O$, $M_r = 274{\cdot}92$, $P4_32_12$, $a = 6{\cdot}7803$ (6), $c = 18{\cdot}288$ (2) Å, $V = 840{\cdot}73$ (2) Å^3, $Z = 4$, $T = 295$ K; λ(Mo $K\alpha$) = 0·71069 Å, $\mu = 2{\cdot}553$ mm^{-1}, $F(000) = 544$, $R = 0{\cdot}014$ for 1765 reflections (X-ray); $\lambda = 1{\cdot}210$ Å, $\mu = 0{\cdot}047$ mm^{-1}, $R = 0{\cdot}035$ for 628 reflections (neutron).

1. Introduction

Experimental deformation electron densities of compounds comprising first- and second-row elements are mostly in good qualitative agreement with theoretical deformation maps (reviewed by Feil, 1986). For compounds with heavier elements, however, the picture is less clear. On the theoretical side it is unclear as to what extent the deformation is dominated by crystal-field effects, *i.e.* what exactly should

* Present address: Institut Laue–Langevin, 156X, 38042 Grenoble CEDEX, France.

† Permanent address: Institute of Nuclear Chemistry and Technology, Dorodna 16, 03-195 Warsaw, Poland.

0108-7681/90/010027-13$03.00

a chemical bond to a transition metal look like. On the experimental side the heavier elements lead to more absorption and hence greater uncertainty in the correction, and, because of the larger inert core, to a decreased fraction of the scattering coming from the valence electrons. On the other hand, the contraction of the *d*-electron distribution of the heavier elements of the first transition-metal series gives stronger X-ray scattering at higher angles compared with the valence electrons of the lighter members.

Despite these difficulties quite a number of experimental investigations of the deformation electron density in transition-metal compounds have been performed. For recent reviews see Coppens & Hall (1982), Coppens (1985) and Hall (1986). Of particular relevance to the present work are the few studies of transition-metal salt hydrates: $CuSO_4.5H_2O$ (Varghese & Maslen, 1985), $CrSO_4.5H_2O$ (Vaalsta & Maslen, 1987) and $NH_4M(SO_4)_2.6H_2O$ (M = Mn, Ni, Cu) (Maslen, Ridout & Watson, 1988; Maslen, Watson & Moore, 1988). $ND_4Ni(SO_4)_2.6D_2O$ has also been investigated by polarized neutron diffraction (Fender, Figgis & Forsyth, 1986). The primary interest in these studies was in the electron density around the metal atom and whether it reflected any departure from ideal octahedral geometry of the environment of the metal atom. Little attention was paid to the details of the hydrogen bonding and electron density around the lighter elements, least of all around the water molecules, in the presence of such strong scatterers. The published deformation maps (difference or $X-N$ Fourier syntheses) suffer from many of the experimental difficulties mentioned above. They often contain a lot of spurious peaks, and it seems rather difficult to draw definite conclusions concerning the electron distributions around the metal atoms.

In this paper we present the deformation electron density of the title compound determined from combined X-ray and neutron diffraction data. Our interests in this compound are twofold. First to study the electron density distribution around the Ni atom, and secondly to see if useful details of the deformation of the water molecules can be obtained. As the three crystallographically independent water molecules are coordinated in different ways to the Ni atom, we also have the interesting possibility of comparing the different influences of Ni on the electron densities of these water molecules, specifically in the lone-pair regions. To minimize the effects of experimental noise and avoid the problems of phase uncertainty in difference or $X-N$ Fourier syntheses for this noncentrosymmetric structure, modelling of the electron density deformation by multipole fitting is used.

The structure of the title compound was first determined by Beevers & Lipson (1932). O'Connor & Dale (1966) located the hydrogen positions from two-dimensional neutron diffraction data. The precision of the hydrogen positions was improved by Bargouth & Will (1981), and most recently Stadnicka, Glazer & Koralewski (1987) determined the absolute configuration by X-ray diffraction.

2. Experimental

Slow evaporation at 295 K of a concentrated solution of nickel sulfate in slightly acidic heavy water produced deep-green translucent pyramidal or bipyramidal crystals which exhibited the forms (101) and (001).

X-ray data

Intensity data were collected at room temperature from a truncated, nearly square, pyramidal crystal 0·35 mm high and 0·31 mm along the base edges. To avoid exchange of deuterium for hydrogen the crystal was coated with a thin film of polystyrene. Enraf–Nonius CAD-4 diffractometer, graphite (002) monochromatized Mo $K\alpha$ radiation; cell dimensions determined by least-squares fit to the θ values of 25 centred reflections in the range $11 < \theta < 27°$; a nearly complete hemisphere of reflections with $k > 0$ to $\sin\theta/\lambda = 1{\cdot}03$ Å^{-1} scanned in ω–2θ mode, 8628 reflections measured in total including repeated measurements of six standard reflections; background corrections following Lehmann & Larsen (1974), standard deviations estimated from counting statistics, Lorentz and polarization corrections applied; absorption correction by Gaussian integration using the calculated attenuation coefficient $\mu = 2{\cdot}553$ mm^{-1}, transmission range 0·84–0·86.

The four strongest standard reflections increased steadily in intensity during the course of the measurement, suggesting a decrease in the crystal perfection owing to radiation damage. Recollection of the first shell of reflections ($\theta < 12°$) at the end of the data collection, and comparison of these with the first measurements showed that only the strongest reflections had increased significantly. No reflections beyond the first shell should be affected. Since the average of the elapsed irradiation times at which the pairs of equivalent reflections in the first shell were measured are all about the same, and we can ignore the effect beyond the first shell, averaging equivalent reflections effectively cancels the effects of the time dependence of the radiation damage even for the strongest reflections. Averaging of the 6571 equivalent reflections (standard reflections omitted) in the Laue group 422 gave 1867 independent reflections with an agreement index, $[\sum w(|F_o|^2 - \langle|F_o|^2\rangle)^2/\sum w|F_o|^4]^{1/2}$, of 0·028; here w is the inverse variance of the observed squared structure amplitude $|F_o|^2$,

and $\langle|F_o|^2\rangle$ is the average of $|F_o|^2$ for each set of equivalent reflections. The time-wise variation of extinction is not the major contribution to this figure; the index increased slightly to 0·030 when only the strongest 10% of the reflections were included.

Neutron data

The positional and thermal parameters of the H atoms used in deformation analyses are usually taken from a neutron diffraction experiment. Unless an accurate correction can be made for the large absorption of neutrons by hydrogen, the hydrogen is often replaced by deuterium for both the X-ray and the neutron experiments. Since both the previous neutron diffraction studies were made on relatively large non-deuterated crystals and no corrections for absorption were made we repeated the neutron experiment on a deuterated sample.

The crystal used for the neutron data collection was a 5·5 mm high truncated bipyramid with a base $4·8 \times 3·2$ mm^2. To avoid exchange the crystal was mounted in a quartz tube. The data were measured on the Aracor–Huber four-circle diffractometer at the R2 reactor at Studsvik, Sweden, in a beam of wavelength 1·210 Å obtained by reflection from a Cu (220 plane) double monochromator. The cell dimensions agreed with the X-ray determined values; complete set of 724 unique reflections with $h \geq k$, $k \geq 0$ and $l \geq 0$ to $\sin\theta/\lambda = 0·68$ Å^{-1} scanned, ω–2θ step scans; three standard reflections measured at regular intervals showed no significant variation. Background corrections following Lehmann & Larsen (1974) and Lorentz corrections applied; absorption correction by Gaussian integration using an experimentally determined attenuation coefficient $\mu = 0·047$ mm^{-1}, transmission range 0·85–0·90.

All data reduction programs and the full-matrix least-squares program *UPALS* used for structure refinement have been described by Lundgren (1982).

3. Refinements

The atomic positions of O'Connor & Dale (1966) were used as starting values in the refinements. In both the neutron and X-ray refinements the quantity minimized was $\sum w(|F_o|^2 - |F_c|^2)^2$, where $w^{-1} = \sigma^2_{\text{count}}(|F_o|^2) + k^2|F_o|^4$ and σ_{count} was derived from Poisson counting statistics. The constant k was fixed empirically at 0·09 and 0·01 for the neutron and X-ray data, respectively, on the basis of weighting analyses for different values of k.

Neutron data

The scattering lengths used were 1·0300, 0·2847, 0·5803 and 0·6674 cm^{-12} for Ni, S, O and D, respectively (Sears, 1986). Several extinction models within the Becker & Coppens (1974) formalism were tried: type I, type II or general, isotropic or anisotropic (Thornley & Nelmes, 1974), with Gaussian or Lorentzian mosaic-spread distributions. All refinements indicated severe extinction for many reflections.

As mostly found for neutron data the best agreement between observed and calculated data was for an isotropic type-I model with a Lorentzian mosaic-spread distribution. Only the 628 reflections with $|F_o|^2 \geq 3\sigma(|F_o|^2)$ and suffering less than 75% extinction were used in the final refinement. The 112 variable parameters were the scale factor, the angular mosaic width, the positional and anisotropic thermal parameters of all atoms, and the proportion of deuterium content to hydrogen content (assumed to be the same for the three independent sites). The agreement indices, as defined in Table 1, following the final refinement were $R = 0·039$, $wR = 0·105$ and $S = 1·18$. The final fractional atomic coordinates and equivalent isotropic displacement parameters are given in Table 2. The refined deuterium-to-hydrogen content corresponded to 96·6 (4)% exchange.

Table 1. *X-ray refinement details*

I, conventional refinement. II, deformation refinement, 432 symmetry assumed for Ni, $\bar{4}3m$ symmetry assumed for S, sulfate O atoms equivalent, water molecules equivalent, *mm*2 symmetry assumed for the water O atoms. III, deformation refinement, $\bar{4}3m$ symmetry assumed for S, sulfate O atoms equivalent, water molecules equivalent, *mm*2 symmetry assumed for the water O atoms. IV, deformation refinement, sulfate O atoms equivalent, water molecules equivalent, *mm*2 symmetry assumed for the water O atoms. V, deformation refinement, water molecules equivalent, *mm*2 symmetry assumed for the water O atoms. VI, deformation refinement, *mm*2 symmetry assumed for the water O atoms, water D atoms equivalent. VII, deformation refinement, water D atoms equivalent. $\Delta = |F_o|^2 - |F_c|^2$.

	I	II	III	IV	V	VI	VII
n (No. of reflections)	1765	1765	1765	1765	1765	1765	1765
p (No. of parameters)	57	93	108	121	151	179	197
$R = \sum\|\Delta I\|/\sum F_o^2$	0·0268	0·0171	0·0165	0·0157	0·0152	0·0144	0·0150
$wR = (\sum w\Delta^2/\sum wF_o^4)^{1/2}$	0·0585	0·0305	0·0300	0·0282	0·0251	0·0240	0·0238
$S = [\sum w\Delta^2/(n-p)]^{1/2}$	3·722	1·965	1·937	1·830	1·643	1·585	1·578
No. of reflections with $\|\Delta I\|/\sigma > 4·0$	257	80	64	49	20	16	18

X-ray data

Only the 1765 reflections with $|F_o|^2 \geq 3\sigma(|F_o|^2)$ were used. Two sets of refinements were carried out: (*a*) a conventional refinement assuming spherical atomic scattering factors, and (*b*) deformation refinements in which the aspherical valence-electron distribution was fitted to multipole deformation functions. In both sets of refinements the spherical scattering factors for Ni, S and O were the neutral-atom relativistic Hartree–Fock scattering factors of Doyle & Turner (1968), while the non-relativistic Hartree–Fock scattering factor of H (Cromer & Mann, 1968) was assumed for D. The anomalous-dispersion contributions were from Cromer &

Table 2. *Fractional atomic coordinates and equivalent isotropic displacement parameters* ($Å^2$) *for* $NiSO_4.6D_2O$ *at* 295 K (*upper figures, neutron refinement; lower figures when given, X-ray refinement* VI)

The form of the displacement factor was $\exp(-2\pi^2\sum_i\sum_j U_{ij}\mathbf{h}_i\mathbf{h}_j a_i^* a_j^*)$; $U_{eq} = (U_{11} + U_{22} + U_{33})/3$.

	x	y	z	U_{eq}
Ni	−0·2104 (1)	−0·2104	0·0	0·0095 (3)
	−0·21039 (2)	−0·21039	0·0	0·0146 (0)
S	−0·7090 (4)	−0·7090	0·0	0·0101 (9)
	−0·70910 (5)	−0·70910	0·0	0·0167 (0)
O(1)	−0·1726 (3)	0·0469 (3)	−0·05257 (10)	0·0229 (6)
	−0·17284 (8)	0·04673 (13)	−0·05278 (3)	0·0301 (1)
O(2)	−0·4701 (2)	−0·2442 (2)	−0·05628 (10)	0·0159 (5)
	−0·47011 (13)	−0·24399 (6)	−0·05617 (2)	0·0225 (1)
O(3)	−0·0655 (2)	−0·3568 (2)	−0·08475 (9)	0·0150 (5)
	−0·06596 (13)	−0·35637 (7)	−0·08493 (2)	0·0213 (1)
O(4)	−0·6217 (3)	−0·6205 (3)	−0·06589 (9)	0·0255 (6)
	−0·61965 (22)	−0·62012 (16)	−0·06604 (5)	0·0318 (2)
O(5)	−0·9229 (2)	−0·6725 (3)	−0·00020 (11)	0·0228 (5)
	−0·92339 (14)	−0·67230 (14)	−0·00050 (7)	0·0287 (1)
D(11)	−0·0776 (3)	0·1459 (3)	−0·04018 (12)	0·0272 (6)
D(12)	−0·2489 (3)	0·0839 (3)	−0·09466 (9)	0·0295 (6)
D(21)	−0·5666 (3)	−0·1433 (3)	−0·04725 (12)	0·0306 (6)
D(22)	−0·5347 (3)	−0·3723 (3)	−0·05872 (11)	0·0254 (5)
D(31)	0·0144 (3)	−0·4643 (3)	−0·06653 (12)	0·0296 (5)
D(32)	0·0160 (2)	−0·2716 (3)	−0·11624 (10)	0·0253 (5)

Liberman (1970). A number of extinction models within the Becker & Coppens (1974) formalism were tried. Again an isotropic type-I correction was found to be most appropriate. In all refinements the deuterium positional parameters were fixed to the values refined from the neutron data.

(*a*) *Conventional refinement*. The following parameters were refined: the scale factor, the mosaic width, and the positional and anisotropic displacement parameters of all atoms other than the D atoms. Initially the deuterium displacement parameters were fixed to the values refined from the neutron data.

For crystals in polar space groups it is possible to determine the absolute configuration if the anomalous-scattering contributions, as in this case, are sufficiently large. Refinements were therefore carried out in both of the enantiomorphic space groups $P4_12_12$ and $P4_32_12$; the initial coordinates were those of O'Connor & Dale (1966), with the signs retained in $P4_12_12$, or reversed in $P4_32_12$. Unlike the crystal studied by Stadnicka *et al.* (1987) our crystal had clearly grown in the $P4_32_12$ enantiomorph ($wR = 0{\cdot}14$ in $P4_12_12$; $wR = 0{\cdot}04$ in $P4_32_12$).

It is frequently observed in combined X-ray and neutron studies that the X-ray refined coordinates for atoms other than D agree satisfactorily well with the neutron coordinates but that the displacement parameters are systematically higher in the X-ray case. Possible causes of this discrepancy are thought to be thermal diffuse scattering, different systematic errors in the background correction (Coppens, Boehme, Price & Stevens, 1981), multiple diffraction (Lundgren, 1980) or inappropriate atomic scattering factors (Larsen & Hansen, 1984). A disagreement was also observed in the present study, the average discrepancy for the O atoms being 38 (8)% for both conventional and deformation refinements. In our case the disagreement between X-ray and neutron parameters cannot be due solely to errors in experimental technique, since the average disagreement over the heavy atoms between our X-ray displacement parameters and those of Stadnicka *et al.* (1987) is only 2%, and the average disagreement over all atoms between our neutron displacement parameters and those of Bargouth & Will (1981) is only 10%. Whatever the cause, the consequence is that the X-ray displacement parameters of the heavy atoms must be refined to avoid unduly large systematic errors in the refinement and final Fourier maps. The deuterium displacement parameters, which cannot be refined with confidence from the X-ray data, were fixed to the neutron values multiplied by 1·38.

As can be seen from Table 1, the final agreement indices for the conventional refinement in $P4_32_12$ are reasonably small; however, Fourier difference syntheses calculated after this refinement clearly showed residual features which should be amenable to modelling by a multipole expansion of the charge distribution of the valence electrons.

(*b*) *Deformation refinement*. To model the aspherical electron distributions we used the multipole deformation functions proposed by Hirshfeld (1971) with modifications by Harel & Hirshfeld (1975) and Hirshfeld (1977). The spherical charge density at each atomic site is modified by an expansion of up to 35 terms, of the general form,

$$\rho_n(r,\theta_k) = N_n r^n \exp(-\gamma r^l)\cos^n\theta_k$$

centred on the site, where r and θ_k are polar coordinates in the kth of a chosen set of axes, n and k are integers [$n = 0, 1, 2, 3$; $k = 1,\ldots (n+1)(n+2)/2$], N_n are normalizing factors, and $l = 1$ or 2 for Lorenztian or Gaussian radial functions, respectively. The scattering factor for each atom is then,

$$f = f_s + \sum C_i\varphi_i$$

where f_s is the spherical free-atom scattering factor, and φ_i are the Fourier transforms of the expansion of the deformation density. The (population) parameters C_i are refinable.

A series of deformation refinements were performed. In the first, the ideal local symmetries of 432 and $\bar{4}3m$ were imposed on the Ni and S atoms, respectively. All water molecules were assumed to be identical with local symmetry $mm2$, while cylindrical symmetry was imposed about the D atoms along the O—D bonds. The independent sulfate O atoms were also assumed to be equivalent with local symmetry

$3m$. These constraints were relaxed successively in the later refinements as indicated in Table 1 together with the final agreement indices for each refinement. The deformation functions of the six independent D atoms were constrained to be identical in each refinement since it was assumed that the differences in the electron density in the O—D bonds would be modelled by the deformation functions on the O atoms. Strong correlation effects meant that the parameter γ, which governs the breadth of the radial function, could not be refined with the other deformation parameters. It was therefore fixed, somewhat arbitrarily, at 3·5 for all atoms. This choice and our assumption of Gaussian radial functions appears reasonable as judged by the flatness of the residual maps after the final refinement. In all refinements the structural model was constrained to be neutral.

The successive improvements in agreement as the constraints are relaxed are significant, except for relaxation of the *mm*2 symmetry on the water O atoms. We also note the relatively small improvement that relaxing the constraint of octahedral symmetry for Ni gives. We shall henceforth consider only the results of refinement VI. The positional and equivalent isotropic displacement parameters of the Ni, S and O atoms following refinement VI are given in Table 2.* The final coordinates of the heavy atoms from the neutron and X-ray refinements agree within three estimated standard deviations (e.s.d.'s) with each other and with those reported by Stadnicka *et al.* (1987). Our X-ray displacement parameters for the heavy atoms also agree within three e.s.d.'s with their values.

4. Deformation maps

$X-N$ syntheses with the observed structure factors assigned the phases of the calculated (N) structure factors underestimate the deformation density for noncentrosymmetric structures (Coppens, 1974). $X-N$ syntheses, in which the observations are assigned phases calculated in a deformation refinement, should not underestimate the density, and have the desirable feature that the observed intensities are still included (Thomas, 1978). There are, however, some disadvantages to these syntheses. The subtraction of the anomalous-dispersion contributions from the observed structure factors is only approximate; for transition metals the contributions can be comparable with the deformation terms. The maps are also sensitive to noise and large absolute errors in the measured structure factors. In particular, extinction-affected and omitted reflections can cause significant distortion. Finally the maps are necessarily a superposition of the deformation functions of all atoms in the unit cell, which may confuse the interpretation of the deformation of a particular atom or molecule. Deformation model maps derived from the fitted multipole model are much less sensitive to noise, insensitive to omitted reflections, and, as proposed below, the effects of superposition can be removed by including only the deformation functions of the constituent of interest. Calculation of the model map is effected in practice by Fourier transformation of a *complete* set of structure factors calculated with f_s and the atomic dispersion corrections set to zero.

To characterize the hydrogen bond it is often useful to apply one of the well-known partitioning schemes in which the total interaction is decomposed into electrostatic, polarization, charge transfer, exchange and dispersion contributions. The different contributions can be defined by various products of the wavefunctions of the isolated constituents and the final complex (*e.g.* Morokuma, 1971), and can also be related to the electron density distribution (Yamabe & Morokuma, 1975). The electrostatic contribution corresponds to the effect that would result if the free constituents, in some hypothetical way, were brought together into the relative positions that they occupy in the actual complex without any deformation of the original charge distributions and without electron transfer. Thus for the water molecule the electrostatic contribution just corresponds to reorientation of the molecule. The polarization contribution corresponds to deformation of the charge distributions of the constituents, still without charge transfer. The other contributions all involve transfer of charge between constituents. It has been shown theoretically that the electrostatic part alone ('the simple electrostatic model') to a first approximation gives a very good representation of the charge distribution in a hydrogen bond (Yamabe & Morokuma, 1975), and that the polarization contribution, the dominant remaining component, is an order of magnitude smaller for weak O—H···O interactions of the type considered here.

We could also apply such a partitioning scheme to other interactions, although the relative importance of the contributions may differ from that for hydrogen bonds, and the difficulty in partitioning the electron distribution between the constituents of a strong interaction means that the analysis should be restricted to weak and moderately strong interactions. We will consider specifically the relatively weak Ni···O bonds between Ni and the water mol-

* Tables of the observed and calculated X-ray structure factors and the anisotropic displacement parameters following the neutron refinement and the final X-ray deformation refinement have been deposited with the British Library Document Supply Centre as Supplementary Publication No. SUP 52323 (19 pp.). Copies may be obtained through The Executive Secretary, International Union of Crystallography, 5 Abbey Square, Chester CH1 2HU, England.

ecules. For the single Ni atom the electrostatic contribution corresponds to orientation within the crystal field of the ideal octahedral charge distribution of the isolated atom, and would be expected to dominate the deformation density.

In an experimental study it is impossible to isolate all five contributions from each other, although some separation, particularly of the electrostatic component from the others, could perhaps be made by inspection of the local symmetry of the experimental deformation density, or by comparison of crystallographically independent molecules in the same structure. In $NiSO_4.6D_2O$ we can look for deviations of the Ni deformation from ideal octahedral symmetry, for deviations of the water molecules from *mm*2 symmetry, and for differences amongst the independent water molecules. However, as we have already pointed out, interpretation of the deformation of a particular atom or molecule in the electron density maps based on all atoms in the unit cell may be confused by the superposition of the deformation functions of neighbouring atoms.

We will therefore compare the deformation densities based on the deformation functions of the whole structure with those based on only the deformation functions of the Ni atom or the individual water molecules. In this way the effects of simple superposition on the deformation densities of adjacent constituents may be removed, and an interpretation within the partitioning scheme attempted. The validity of the separation of the deformations of adjacent constituents depends very much on whether the radial functions are appropriate. However, provided we do not attempt to separate strongly covalently bonded atoms, *e.g.* O and D in the water molecules, the region of overlap of the deformation functions where we make the separation should occur in the tails of the radial functions of the individual atoms or molecules, and the choice of radial function and exponents should not be too critical. A closer analysis of this point with a comparison with the theoretical densities of truly isolated constituents will be made elsewhere.

5. Results and discussion

For a general description of the crystal structure we refer to the earlier reports (Beevers & Lipson, 1932; Stadnicka *et al.*, 1987). Selected bond lengths and angles are listed in Table 3, including more precise values than quoted in earlier studies for the water molecules and hydrogen bonds.

Nickel is located on a 4(*a*) site with symmetry 2. The surrounding six water O atoms form a slightly distorted octahedron, in which O(3) and O(3′) are located on opposite corners, whereas O(1) and O(1′), and similarly O(2) and O(2′), are adjacent to one another. For the following discussion it is important to note that the three independent water molecules are coordinated to nickel in quite different ways (*cf.* Fig. 1 and Table 3):

(*a*) Water 1 has an almost perfect planar trigonal environment. The deviation of nickel from the water plane is only 1°, Fig. 1(*a*). Furthermore it donates one hydrogen bond to the water O(3) atom and one to the sulfate O(5) atom.

(*b*) Water 2 is also surrounded by only three neighbours but in this case nickel approaches the water O atom in a tetrahedral rather than trigonal direction with respect to the protons [the angle to the water plane is 36°, Fig. 1(*b*)]. There is, however, no neighbour in the fourth tetrahedral direction. The water molecule donates one hydrogen bond to the sulfate O(4) atom and one to the sulfate O(5) atom.

(*c*) Water 3, by contrast, has a complete tetrahedral environment. It receives a coordinative bond from Ni [angle of 47° to the water plane, Fig. 1(*c*)] and a hydrogen bond from water 1 (angle of 58° to

Table 3. *Selected bond lengths* (Å) *and angles* (°) *for* $NiSO_4.6D_2O$ *at* 295 K (*neutron diffraction data*)

Standard deviations are given in parentheses. Superscripts on the atom symbols denote equivalent positions: (i) $y, x, -z$; (ii) $y, -1+x, -z$; (iii) $-1+x, y, z$; (iv) $-1+x, -1+y, z$; (v) $\frac{1}{2}-x, \frac{1}{2}+y, \frac{1}{4}-z$.

(*a*) Covalent bonds			
Ni—O(1)	2·009 (2)	O(1)—Ni—O(2)	88·10 (8)
Ni—O(2)	2·052 (2)	O(1)—Ni—O(3)	89·86 (8)
Ni—O(3)	2·086 (2)	O(1)—Ni—O(1′)	90·43 (14)
		O(1)—Ni—O(3′)	90·41 (8)
		O(2)—Ni—O(3)	88·79 (8)
		O(2)—Ni—O(2′)	93·39 (12)
		O(2)—Ni—O(3′)	91·95 (8)
		O(1)—Ni—O(2′)	178·32 (9)
		O(3)—Ni—O(3′)	179·61 (12)
S—O(4)	1·470 (3)	O(4)—S—O(5)	109·04 (12)
S—O(5)	1·472 (3)	O(4)—S—O(4′)	110·09 (34)
		O(4)—S—O(5′)	109·65 (11)
		O(5)—S—O(5′)	109·35 (34)
(*b*) Water molecules			
O(1)—D(11)	0·957 (3)	D(11)—O(1)—D(12)	111·7 (3)
O(1)—D(12)	0·961 (3)		
O(2)—D(21)	0·961 (3)	D(21)—O(2)—D(22)	109·7 (3)
O(2)—D(22)	0·974 (3)		
O(3)—D(31)	0·967 (3)	D(31)—O(3)—D(32)	109·2 (2)
O(3)—D(32)	0·986 (3)		
(*c*) Hydrogen bonds			
O(1)···O(5^{iv})	2·721 (3)	O(1)—D(11)···O(5^{iv})	168·9 (2)
D(11)···O(5^{iv})	1·775 (3)		
O(1)···O(3^{v})	2·797 (3)	O(1)—D(12)···O(3^{v})	169·6 (2)
D(12)···O(3^{v})	1·847 (3)		
O(2)···O(5^{ii})	2·774 (3)	O(2)—D(21)···O(5^{ii})	155·4 (2)
D(21)···O(5^{ii})	1·871 (3)		
O(2)···O(4)	2·756 (3)	O(2)—D(22)···O(4)	172·4 (2)
D(22)···O(4)	1·788 (3)		
O(3)···O(5^{iii})	2·812 (3)	O(3)—D(31)···O(5^{iii})	154·3 (2)
D(31)···O(5^{iii})	1·909 (3)		
O(3)···O(4^{v})	2·735 (3)	O(3)—D(32)···O(4^{v})	168·8 (2)
D(32)···O(4^{v})	1·761 (3)		

the water plane). Two hydrogen bonds are donated to the sulfate O(4) and O(5) atoms.

The free Ni^{2+} ion has a d^8 electron configuration. An Ni^{2+} ion octahedrally coordinated by a weak ligand field (spin-free state) has a symmetrical $d_\varepsilon^6 d_\gamma^2$ electronic configuration with two electrons in each of the three d_ε orbitals and one electron in each of the two d_γ orbitals. In a strong ligand field, however, both d_γ electrons occupy the d_z^2 orbital, and the $d_{x^2-y^2}$ orbital is unoccupied. In the latter case the repulsion of the ligands by the electrons in the d_z^2 orbital will lead to a square-planar arrangement of the ligands, as commonly observed in Ni^{2+} complexes with strong ligands.

In the present case, with water as a rather weak ligand, we expect a spin-free state for Ni^{2+} and thus regular octahedral coordination, *provided* that all six ligand water molecules are coordinated in an equivalent way. We have already noted, however, that the three water molecules are attached quite differently. These differences are reflected in the Ni—O distances within the coordination sphere of nickel: Ni—O(3) is 0·04 Å longer than Ni—O(2), which in turn is 0·04 Å longer than Ni—O(1) (see Table 3). The coordination octahedron is thus elongated in the O(3)—Ni—O(3′) direction as expected from the differences in the water coordination described above. This elongation might be taken as a slight tendency towards a square-planar arrangement around Ni^{2+}. However, it seems more likely that the formation of directed hydrogen bonds around the water molecules has forced the molecules to approach nickel in different ways, with the different Ni—O distances as a secondary result. That the hydrogen-bond formation might play a dominant role is supported by the similar hydrogen-bond lengths (2·72–2·81 Å) and the much smaller variation in hydrogen-bond angle amongst the six bonds than in the angles made by Ni to the water planes.

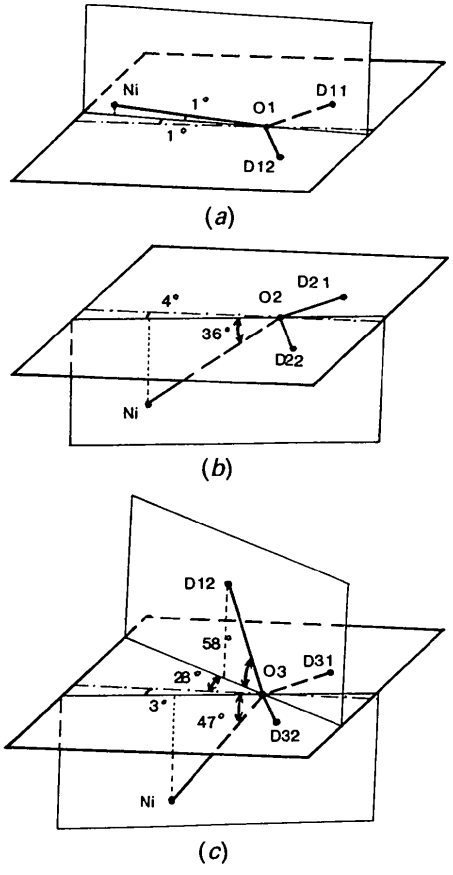

Fig. 1. Nearest-neighbour geometries of the three unique water O atoms: (*a*) O(1), (*b*) O(2), (*c*) O(3).

Deformation electron densities

The static multipole model deformation maps for the sections of interest around Ni and around the three water molecules after refinement VI are illustrated in Figs. 2 and 3, respectively. In the diagrams the three atoms defining each section are written without parentheses. For orientation purposes other atoms close to these sections and the relevant H atoms are indicated within parentheses. In an attempt to distinguish the characteristic features of the Ni ion and the water molecules, the maps calculated from only the deformation functions of each of these constituents are also plotted separately.

(*a*) *The* Ni *atom.* Let us first consider the total deformation maps (Figs. 2*a–c*). Apart from the large negative peak centred on Ni, the only definite feature observed is an electron deficiency in the bonds to the surrounding water O atoms in comparison with the diagonal directions. This is just the feature expected for a $d_\varepsilon^6 d_\gamma^2$ electron configuration, where the diagonally directed d_ε orbitals (d_{xy}, d_{xz} and d_{yz}) are all completely full while the two d_γ orbitals share two electrons. The deformation distribution is not so clearly defined, however, that we can state how the d_γ orbitals share the electrons, *i.e.* whether the Ni deformation is ideally octahedral.

The deformation maps of Ni with the adjacent water deformation functions omitted (Figs. 2*a′–c′*) give a much clearer picture of the Ni electron density. The electron deficient peaks in the three independent Ni—O directions now appear more or less equivalent; likewise for the positive peaks in the diagonal directions. These observations agree with a spin-free configuration with both d_γ orbitals half-full as opposed to the spin-paired alternative with d_{z^2} full and $d_{x^2-y^2}$ empty. The deformation thus has nearly ideal octahedral symmetry, even though only the crystallographic site symmetry 2 was imposed on the Ni deformation functions in the refinement. More-

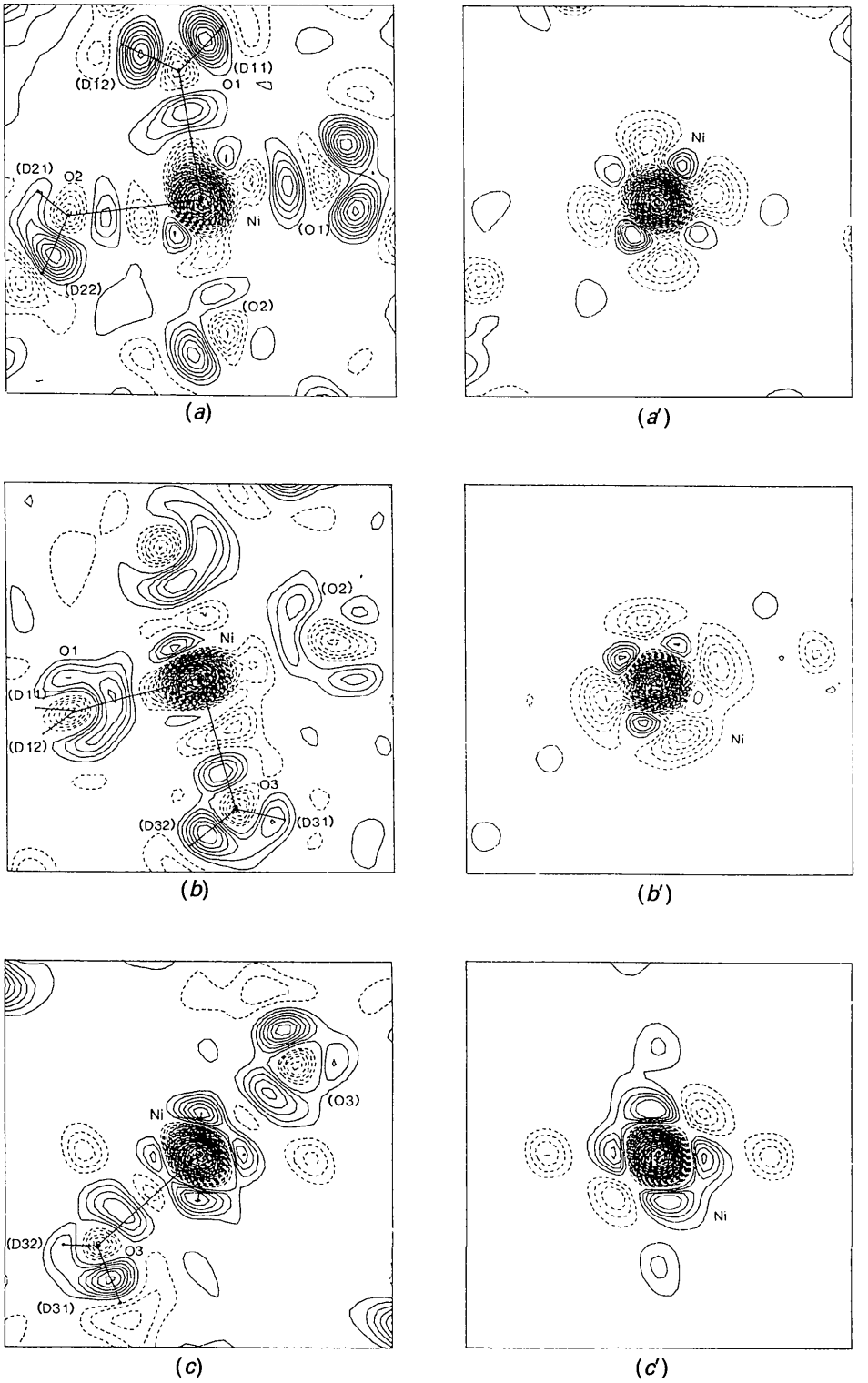

Fig. 2. $Ni(D_2O)_6$ static deformation model maps based on a full set of reflections to $\sin\theta/\lambda = 1{\cdot}03$ Å^{-1}. (All maps in Figs. 2–4 are based on refinement VI.) Maps (*a*) and (*a'*) are calculated in the plane through Ni, O(1) and O(2), (*b*) and (*b'*) in the plane through Ni, O(1) and O(3), and (*c*) and (*c'*) in the plane through Ni, O(3) and the internal bisector of O(1)···Ni···O(2). All atoms are included in the calculation of the unprimed maps, while only the Ni deformation functions are included in the calculation of the primed maps. Contours are drawn at intervals of 0·05 e Å^{-3}. Negative contours are dashed; the zero-level contour is omitted. The map (not shown) through Ni, O(3) and the external bisector of O(1)···Ni···O(2) calculated using only the Ni deformation functions is very similar to (*c'*).

over, the angles between the vectors from Ni to the negative peaks are closer to 90° than the angles between the Ni—O vectors (Table 3). Our earlier suggestion that the elongation of the bonds along Ni—O(3) results primarily from the particular approach of the water molecules rather than from repulsion of $D_2O(3)$ by preferential occupation of the Ni d_{z^2} orbital is thus supported by the electron density analysis. The maxima along the eight diagonal directions lie at distances 0·6–0·7 Å from the nucleus, which compare well with the 0·6 Å calculated for the Ni atom in the similarly weak octahedral field in NiO (Watson & Freeman, 1960). The six minima in the bond directions lie at distances 0·7–0·8 Å.

Our total deformation maps (Figs. 2*a–c*) show a distortion from ideal octahedral symmetry in the distribution around Ni, which is very similar to the distortion observed by Maslen, Ridout & Watson (1988) in $X-N$ maps of $NH_4NiSO_4.6H_2O$ and which they attribute to the nearly planar geometry of the second coordination sphere of Ni. Our individual maps (Figs. 2*a′–c′*) show, however, that the distortion in the total distribution is due primarily to superposition of the ligands in a non-ideal geometry on an ideally octahedral Ni^{2+} deformation. The comparatively slight improvement in agreement from refinements II to III also suggests an ideally octahedral deformation of the Ni^{2+} electron density. Could the distortion observed by Maslen, Ridout & Watson (1988) in the $X-N$ maps also be due to superposition in a non-ideal geometry, and not to long-range interactions as they have postulated? We note that the polarized neutron diffraction study of $ND_4NiSO_4.6D_2O$ (Fender *et al.*, 1986) implied that the d_γ orbitals in this compound are equivalent.

(*b*) *The water molecules.* The deformation densities are illustrated both in the planes of the water molecules and perpendicular to these, through the two-fold axes, both with all deformation functions included in the calculation (Figs. 3*a–f*), and with only the deformation functions of oxygen and deuterium of the water molecule in question included (Figs. 3*a′–f′*).

We first consider the total maps (Figs. 3*a–f*). The densities in the O—H bond directions of all three molecules are very similar: concentration of density within the bond and deficiency further out. In the region of the 'lone pairs' the deformation density has a very clear banana shape; it is quite concentrated in the plane of the water molecule but very extended perpendicular to this plane, and in general agrees with theoretical calculations (Hermansson, 1984). Very slight excesses just in the lone-pair directions can be observed, but there are also further peaks near the O atoms that confuse interpretation of the bonding deformation. All these features, including the rather irregular contours in the lone-pair plane, are typical for experimental deformation maps of water molecules.

Of particular interest here is the possible influence of the environment on the lone-pair distribution, first of all owing to the coordination to Ni, and for $D_2O(3)$, also owing to the hydrogen bond donated by $D_2O(1)$ (*cf.* Hermansson, Olovsson & Lunell, 1984). Our total deformation map for $D_2O(3)$, for example, shows a slightly smaller lone-pair peak in the direction of Ni than in the direction towards $D_2O(1)$ (Fig. 3*f*). Experimental studies of other hydrates give rather contradictory results; in some cases the lone-pair peak becomes more pronounced when the O atom is approached by a metal ion or receives a hydrogen bond, in other cases the opposite effect is observed (*e.g.* Eisenstein & Hirshfield, 1983). The observed decrease in the lone-pair density in the shortest hydrogen bond in $NaHC_2O_4.H_2O$ (Delaplane, Tellgren & Olovsson, 1990) is also predicted by *ab initio* calculation of the total density, but Lunell (1984) has shown that the theoretical result is an artifact due to superposition of the donor and acceptor deformation densities. Perhaps the other apparently contradictory experimental observations are also due to superposition of the deformation distributions of neighbouring atoms.

Our total deformation maps also suggest that there is distortion in the plane of the water molecule as well as in the lone-pair plane. For example the lone-pair density of $D_2O(1)$ in the water plane is compressed quite significantly in the direction of Ni (Fig. 3*a*).

We now turn to the individual deformation maps of the water molecules (Figs. 3*a′–f′*). These maps are unusually free of spurious peaks and look much more like the theoretical density of a free water molecule (Hermansson, 1984) than do the total maps. A notable difference compared to the free molecule is a decrease in resolution of the lobes in the lone-pair region.

Comparing the individual maps with the total maps we see immediately that many of the lone-pair 'features' in the total maps have resulted simply from superposition of the densities of the separate units. For example the compression of the lone-pair density in the plane of $D_2O(1)$ in the total deformation map is due to the contribution of the negative region of Ni coordinated in this direction (compare Fig. 3*a* with Fig. 3*a′* and Fig. 2*a′*). The same effect occurs in the lone-pair plane (compare Figs. 3*b* and 3*b′*).

An approaching hydrogen bond has a similar effect to that observed for Ni, as illustrated by the O1—D(12)···O(3) bond in Fig. 4(*a*) (total deformation map) and Fig. 4(*a′*) (juxtaposed individual deformation maps). In the total deformation map the lone-pair density of O(3) in the direction of the

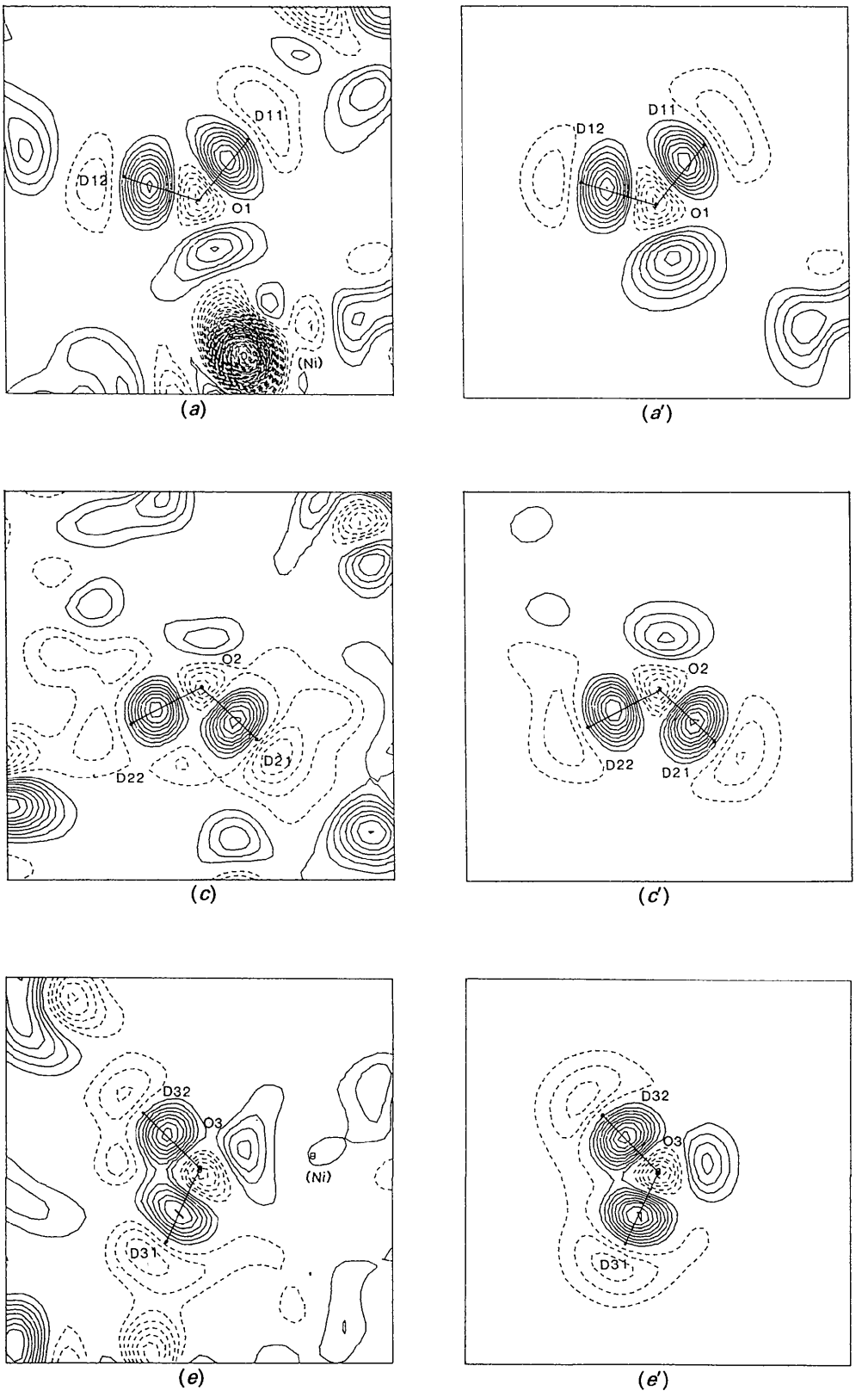

Fig. 3. Static deformation model maps in and perpendicular to the planes of the three unique water molecules. (*a*), (*c*) and (*e*) are calculated in the plane of the water molecules 1, 2 and 3, respectively; (*b*), (*d*) and (*f*) perpendicular to the respective planes.

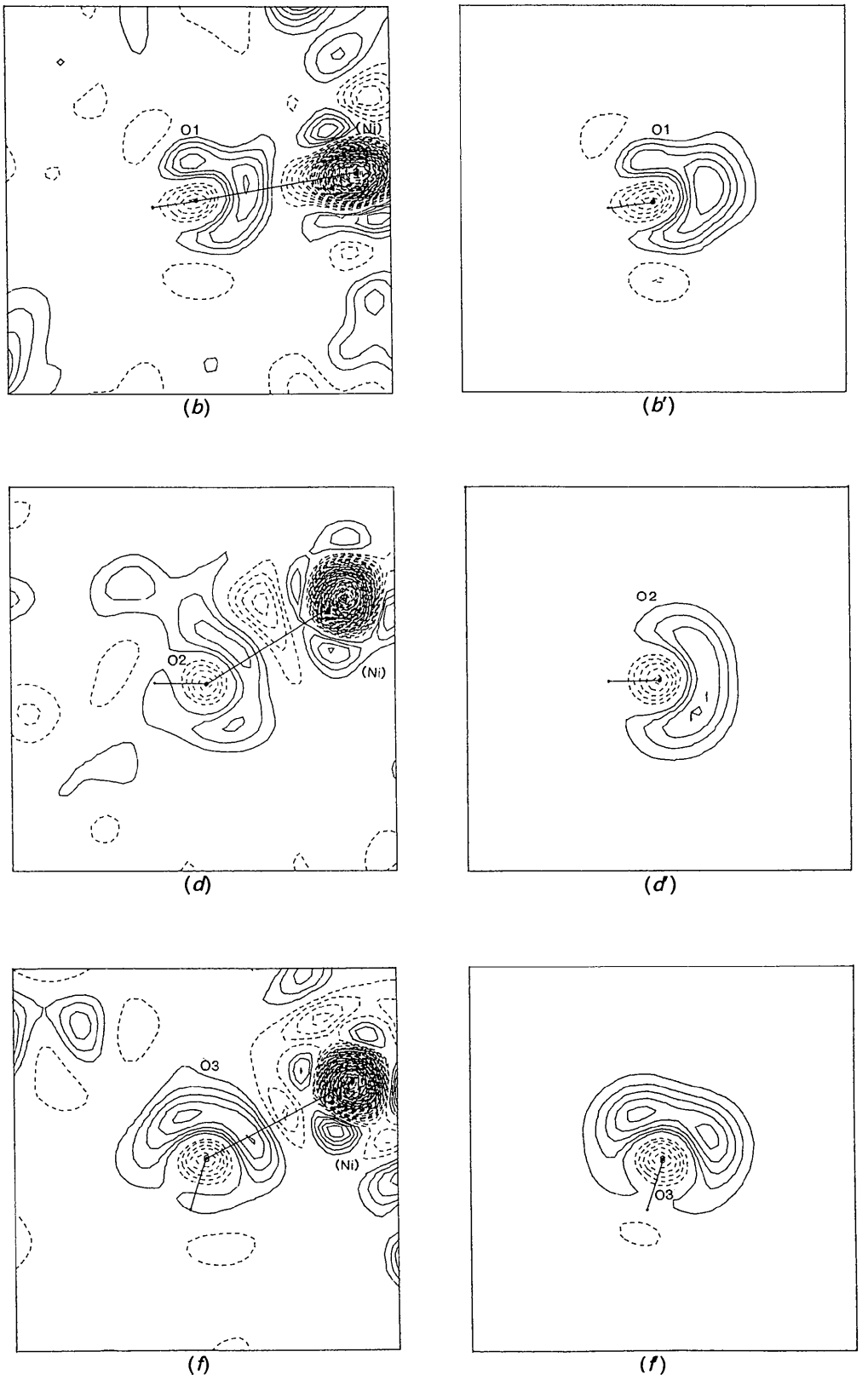

Fig. 3 (*cont.*) All atoms are included in the calculation of the unprimed maps; only the deformation functions of the O and D atoms of the water molecule in question are included in the primed maps. Reflection limit and contours as in Fig. 2.

hydrogen bond is noticeably decreased and shifted closer to O(3) due to the superposition with negative density from $D_2O(1)$, compared with the individual maps. The effect appears to be somewhat smaller than for the O(1)···Ni bond, however.

A comparison of the deformation densities in the lone-pair region of the three different water molecules in the individual maps now allows us to answer our original question whether the environment distorts the lone-pair system or not. While all three water molecules are very similar in the plane of the water molecule all the lone-pair densities (Figs. 3*b*′, 3*d*′ and 3*f*′) are slightly different. The lone-pair density of O(1) has a single lobe that extends significantly towards Ni, while that of O(3) has two lobes, one extending towards Ni and the other towards D(22). We attribute these differences in the lone-pair densities of O(1), O(2) and O(3) to their different local environments and the polarizing influence of the ligands.

Mirror symmetry in and perpendicular to the plane of the water molecule was imposed in the refinement and this is evident in the individual deformation maps. Relaxing these constraints caused little change in the maps or in the agreement between observed and calculated structure factors (Table 2). It is beyond the accuracy of our data to attempt to interpret differences in the lone-pair lobes on a given water molecule.

The bond peak heights of the three water molecules agree very well in both the total deformation maps and the isolated maps: 0·40, 0·45 and 0·45 e $Å^{-3}$ for the O—D bonds in O(1), O(2) and O(3), respectively; 0·30, 0·20 and 0·22 e $Å^{-3}$ for the lone-pair peaks. The similarity in the strengths of the six hydrogen bonds is reflected in the nearly identical shapes and heights of the corresponding positive and negative peaks near the D atoms in the three molecules. The lower values of the lone-pair peaks of O(2) and O(3) compared with O(1) are consistent with the more diffuse nature of these peaks owing to the nearly tetrahedral local geometries.

6. Concluding remarks

Meaningful interpretation of the deformation density of water molecules can be made in the presence of strong X-ray scatterers such as transition-metal atoms, but multipole fitting and plotting of model deformation maps are preferable to conventional Fourier difference techniques to minimize the effects of noise. Model maps based on just the deformation functions of the individual atoms or molecules may allow the deformation of neighbouring constituents to be separated and remove artifacts caused by superposition.

When the effects of superposition are removed, the deformation electron density of Ni in $NiSO_4.6D_2O$ shows just the features expected in a weak octahedral ligand field. The individual deformations of the three water molecules show that their interaction with the environment is also largely electrostatic; however, some polarization of the lone-pair densities in the different environment is evident.

This work was funded by the Swedish Natural Science Research Council (NFR). We especially thank Dr R. Tellgren for collecting the neutron data.

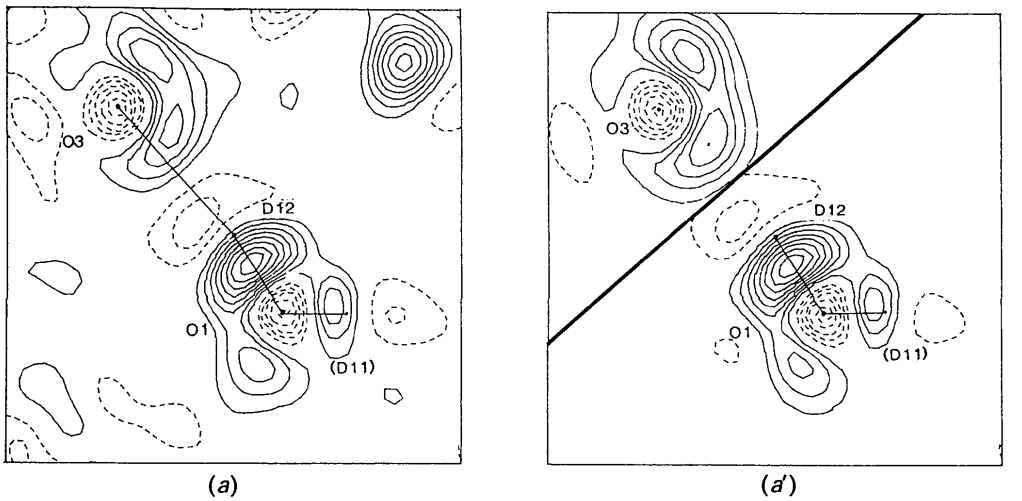

(*a*) (*a*′)

Fig. 4. Static deformation map through O(1)—D(12)···O(3). All atoms are included in the calculation of (*a*); (*a*′) is a composite of the two maps with only the deformation functions of the atoms in $D_2O(1)$ included in the calculation of the region near $D_2O(1)$ and only the deformation functions of O(3) included in the calculation of the region near O(3). The heavy line shows the limit of region. Reflection limit and contours as in Fig. 2.

We also gratefully acknowledge the skillful technical assistance of Mr H. Karlsson and Mr S. Åhlin, and the guidance of Drs J.-O. Lundgren and J. O. Thomas in questions of computational procedure.

References

BARGOUTH, M. O. & WILL, G. (1981). ICTP Report. International Centre for Theoretical Physics, Trieste, Italy.

BECKER, P. & COPPENS, P. (1974). *Acta Cryst.* A**30**, 129–147.

BEEVERS, C. A. & LIPSON, H. (1932). *Z. Kristallogr.* **83**, 123–135.

COPPENS, P. (1974). *Acta Cryst.* B**30**, 255–261.

COPPENS, P. (1985). *Coord. Chem. Rev.* **65**, 285–307.

COPPENS, P., BOEHME, R., PRICE, P. F. & STEVENS, E. D. (1981). *Acta Cryst.* A**37**, 857–863.

COPPENS, P. & HALL, M. B. (1982). Editors. *Electron Distributions and the Chemical Bond*, Sections 5 and 6. New York: Plenum.

CROMER, D. T. & LIBERMAN, D. (1970). *J. Chem. Phys.* **53**, 1891–1898.

CROMER, D. T. & MANN, J. B. (1968). *Acta Cryst.* A**24**, 321–324.

DELAPLANE, R. D., TELLGREN, R. & OLOVSSON, I. (1990). *Acta Cryst.* Submitted.

DOYLE, P. A. & TURNER, P. S. (1968). *Acta Cryst.* A**24**, 390–399.

EISENSTEIN, M. & HIRSHFELD, F. L. (1983). *Acta Cryst.* B**39**, 61–75.

FEIL, D. (1986). *Chem. Scr.* **26**, 395–408.

FENDER, B. E. F., FIGGIS, B. N. & FORSYTH, J. B. (1986). *Proc. R. Soc. London Ser. A*, **404**, 139–145.

HALL, M. B. (1986). *Chem. Scr.* **26**, 389–394.

HAREL, M. & HIRSHFELD, F. L. (1975). *Acta Cryst.* B**31**, 162–172.

HERMANSSON, K. (1984). *Acta Univ. Ups. Nova Acta Regiae Soc. Sci. Ups.* No. 744.

HERMANSSON, K., OLOVSSON, I. & LUNELL, S. (1984). *Theor. Chim. Acta*, **64**, 265–276.

HIRSHFELD, F. L. (1971). *Acta Cryst.* B**27**, 769–781.

HIRSHFELD, F. L. (1977). *Isr. J. Chem.* **16**, 226–229.

LARSEN, F. K. & HANSEN, N. K. (1984). *Acta Cryst.* B**40**, 169–170.

LEHMANN, M. S. & LARSEN, F. K. (1974). *Acta Cryst.* A**30**, 580–584.

LUNDGREN, J.-O. (1980). *Acta Cryst.* B**36**, 1774–1781.

LUNDGREN, J.-O. (1982). *Crystallographic Computer Programs.* Report UUIC-B13-04-05. Institute of Chemistry, Univ. of Uppsala, Sweden.

LUNELL, S. (1984). *J. Chem. Phys.* **80**, 6185–6193.

MASLEN, E. N., RIDOUT, S. C. & WATSON, K. J. (1988). *Acta Cryst.* B**44**, 96–101.

MASLEN, E. N., WATSON, K. J. & MOORE, F. H. (1988). *Acta Cryst.* B**44**, 102–107.

MOROKUMA, K. (1971). *J. Chem. Phys.* **55**, 1236–1244.

O'CONNOR, B. H. & DALE, D. H. (1966). *Acta Cryst.* **21**, 705–709.

SEARS, V. F. (1986). *Methods of Experimental Physics*, Vol. 23*A*, *Neutron Scattering*, edited by K. SKÖLD & D. L. PRICE, pp. 521–550. Orlando: Academic Press.

STADNICKA, K., GLAZER, A. M. & KORALEWSKI, M. (1987). *Acta Cryst.* B**43**, 319–324.

THOMAS, J. O. (1978). *Acta Cryst.* A**34**, 819–823.

THORNLEY, F. R. & NELMES, R. J. (1974). *Acta Cryst.* A**30**, 748–757.

VAALSTA, T. P. & MASLEN, E. N. (1987). *Acta Cryst.* B**43**, 448–454.

VARGHESE, J. N. & MASLEN, E. N. (1985). *Acta Cryst.* B**41**, 184–190.

WATSON, R. E. & FREEMAN, A. J. (1960). *Phys. Rev.* **120**, 1134–1141.

YAMABE, S. & MOROKUMA, K. (1975). *J. Am. Chem. Soc.* **97**, 4458–4465.

Acta Cryst. (1990). B**46**, 39–44

Strukturverfeinerung des Kompositkristalls im mehrdimensionalen Raum

VON KATSUO KATO

*Mukizaishitsu Kenkyusho,** 1-1 *Namiki, Tsukuba-shi, Ibaraki-ken* 305, *Japan*

(*Eingegangen am* 2. *Mai* 1989; *angenommen am* 28. *Juli* 1989)

Abstract

The superspace-group approach formulated for composite crystals by Janner & Janssen [*Acta Cryst.* (1980), A**36**, 408–415] was programmed for computer and applied successfully to the structure refinements of '$LaCrS_3$' ($La_{72}Cr_{60}S_{192}$) [Kato, Kawada & Takahashi (1977). *Acta Cryst.* B**33**, 3437–3443] and $M_{10}Cu_{17}O_{29}$ ($M = Bi_{0.031}Ca_{0.564}Sr_{0.405}$) [Kato, Takayama-Muromachi, Kosuda & Uchida (1988). *Acta Cryst.* C**44**, 1881–1884]. The structure of '$LaCrS_3$' refined to $R = 0.056$ for 2087 reflections and that of $M_{10}Cu_{17}O_{29}$ refined to $R = 0.028$ for 1006 reflections.

* Staatliches Institut für Anorganische Materialforschung (National Institute for Research in Inorganic Materials).

0108-7681/90/010039-06$03.00

Einleitung

Unter einem Kompositkristall versteht man denjenigen Kristall, dessen Struktur aus mehreren ineinandergreifenden Teilen vershiedener Translationsperioden besteht. Jeder einzelne Teil bildet für sich ein system, das Teilsystem, das die Symmetrie einer bestimmten dreidimensionalen Raumgruppe aufweist. Besitzen die Translationsgitter der Teilsysteme eines Kompositkristalls kein gemeinsames dreidimensionales Teilgitter, so ist der Kompositkristall nicht kommensurabel, andernfalls ist er kommensurabel. Im reziproken Raum gibt es Reflexe, die allein von einem einzigen Teilsystem stammen, aber auch diejenigen, zu denen mehrere oder alle Teilsysteme beitragen.